

SciEn Conference Series: Engineering Vol. 3, 2025, pp 181-186

https://doi.org/10.38032/scse.2025.3.46

Numerical Comparison of Laminar Natural Convection Heat Transfer in C-shaped and U-shaped Enclosures

Inkiad Haque Sharar, Md. Mahbubur Rahman and Tanvir Ahmed Fahim*

Department of Mechanical Engineering, Khulna University of Engineering & Technology, Khulna-9203, Bangladesh

ABSTRACT

This research presents a numerical investigation into the influence of natural convection within C-shaped and U-shaped enclosures, employing air as the enclosed fluid. Both shapes are subjected to uniform boundary conditions, with the hot wall and cold rib of the enclosure kept at constant temperature. The outer C-shaped and U-shaped boundary wall is set to a higher temperature compared to the inner one, while the connecting walls between the cold rib and the hot wall are treated as adiabatic. The study assumes a 2-D problem setup, with varying Rayleigh numbers ranging from 10⁴ to 10⁶, ensuring laminar flow conditions across all scenarios. Various aspect ratios (0.3, 0.5, 0.7), the ratio of the outer length to the inner length of the enclosure, are explored in the simulations. Results are depicted through streamline and temperature contour visualizations, revealing the formation of distinct eddies within the enclosures. The analysis highlights an increase in the Nusselt number with a rising Rayleigh number in both enclosures for specific aspect ratios. Besides, a higher Rayleigh number is associated with the formation of more eddies and pronounced changes in the results, particularly evident at a certain aspect ratio. Moreover, the rate of change in the Nusselt number differs between C-shaped and U-shaped enclosures with increasing Rayleigh numbers. From the viewpoint of natural convection, the formation of eddies can modify the temperature gradients and enhance the Nusselt number by boosting heat transfer from the surface to the adjacent fluid. Notably, the study reveals a heightened presence of eddies which ultimately results in a higher Nusselt number at Ra=10⁶.

Keywords: Natural Convection, Aspect Ratio, Laminar Flow, Nusselt Number, Rayleigh Number.



Copyright @ All authors

This work is licensed under a Creative Commons Attribution 4.0 International License.

1. INTRODUCTION

Natural convection occurs in a fluid when some of the fluid particles are heavier than the other particles of the same fluid. The main driving force here is buoyancy. When a fluid surrounds a heat source it absorbs heat, becomes less dense, and rises due to thermal expansion, which is known as free convection. Put another way, bulk fluid movement occurs as lighter components cause denser ones to rise, while heavier components lead to the descent of less dense ones.[1]

Recently, researchers have become attracted in investigating natural convection heat transfer in various enclosures. It is engaged in various technical applications, including geothermal reservoirs, cooling of electric components, solar collectors, and thermal hydraulics in nuclear reactors. The thermal behavior and fluid flow have been analyzed within various enclosures and under different boundary conditions, using fluids like air, water, and nanofluids. Regular cavities are often inadequate for accurately modeling industrial or geophysical systems. Thus, researchers have started studying enclosures such as trapezoidal, C-shaped, L-shaped, U-shaped, and V-shaped [2-6]. for being able to describe every physical phenomenon related to natural convection. Parameters like aspect ratio, inclination angles, Rayleigh numbers, enclosure's shape, and

the fluid used in the enclosure dominate the characteristics of heat transfer characteristics and natural convection inside the enclosure. In 1968, De Vahl Davis[7] investigated the heat transfer characteristics in a two-dimensional rectangular enclosure with varying aspect ratios and Rayleigh numbers. He found that the fluid flow becomes turbulent after a specific Rayleigh number. Rao [8] investigated radiation and convection heat transfer from a rectangular vertical fin array numerically and compared them with experimental data which showed good agreement with each other.

Mahmud et al. [9] observed that increasing the inclination angle of the trapezoidal cavity enhances the convective heat transfer for both shapes, with the trapezoidal cavity showing a more pronounced effect than a square cavity. Jassim[10] found the strength of the flow reduces as the partition thickness increases in a square enclosure at a certain Prandtl number=0.7. Ghalambaz et al [11] determined the heat transfer characteristics effect with varying volume fractions and Rayleigh numbers of nanoparticles by using a nanofluid named Ag-MgO/water in a square enclosure.

Inam [12] studied the change in the convective behavior of natural convection with varying inclination angles and discovered that the heat transfer is improved as the inclination angles increase. Kent[13, 14] has performed several studies related to natural convection. He researched natural convection within isosceles triangular enclosures, exploring different base angles, Rayleigh numbers, and two distinct boundary conditions. For different boundary conditions, different results were observed. Later, he studied triangular-shaped cavities with varying aspect ratios and Rayleigh numbers.

Mahmoodi and Hashemi [3] initiated the study of natural convection in a C-shaped cavity, utilizing Cu-water nanofluid with different volume fractions. They found that the heat transfer rate increased with a decrease in aspect ratio. higher nanoparticle volume fraction, and lower Rayleigh number. Chamkha et al [15] investigated the effect of varying Hartmann number, Rayleigh number, nanofluid volume fraction, and aspect ratio on CuO-water nanofluid under a magnetic field, and found that while the nanoparticle volume fraction boosts natural convection, it also leads to an undesirable increase in the entropy generation rate. Mohebbi et al. [4] investigated the behavior of Al2O3-water nanofluid with varying Rayleigh numbers, nanofluid volume fraction, aspect ratio, and heat source positions within the enclosure. They observed that the Nusselt number increase of the nanofluid was not influenced by the heat source location. For high Rayleigh numbers, the greatest enhancement occurred when the heat source was positioned in the upper section of the vertical. Mahmoodi[16] investigated L-shaped cavities containing Cu nanoparticles, analyzing different aspect ratios, nanofluid volume fractions, and Rayleigh numbers. The study concluded that the heat transfer rate improves as the aspect ratio decreases.

From the previous literature review, it has been found that there is limited research on the effect of aspect ratio when comparing C-shaped and U-shaped enclosures at a considerably low Rayleigh number (Ra $\leq 10^6$) which is the incentive behind conducting the current study. Simulations are performed to investigate laminar natural convection heat transfer in enclosures for three different aspect ratios (AR=0.3, AR=0.5, AR=0.7) of three Rayleigh numbers (Ra = 10^4 , Ra = 10^5 , Ra = 10^6) using ANSYS Fluent 20.2 with air as the working fluid. The flow patterns and temperature distribution within the enclosures are examined by analyzing the streamlines and isotherm contours for each geometry.

2. METHODOLOGY

2.1 Problem statement

C-shaped and U-shaped enclosures are considered in this study with the dimensions as shown in **Fig. 1**. One outer geometry having edge dimensions H and one inner geometry having edge dimensions L and two walls connecting these two geometries have completed the enclosures. The outer geometry is assumed as hot walls having a temperature T_H , the inner geometry is assumed cold walls having a temperature T_C ($T_H > T_C$) and two connecting walls were assumed adiabatic walls for this study. The aspect ratio of this shape can be defined by the ratio of the dimensions of the inner C/U-shape edges to the outer C-shaped and U-shaped edges thus, AR=L/H.

This study concerns two separate environments. Here, C-shaped and U-shaped enclosures are filled with air at various Rayleigh numbers and three different aspect ratios to observe how the Nusselt number varies with AR and Ra. In

both cases, the fluids are Newtonian and incompressible, the flow is two-dimensional and the radiation effects are neglected. The density changes in the fluids are modeled using the standard Boussinesq approximation. All thermophysical properties of the fluids are based on the temperature of the cold wall, set at 300K for this study shown in **Table 1**.

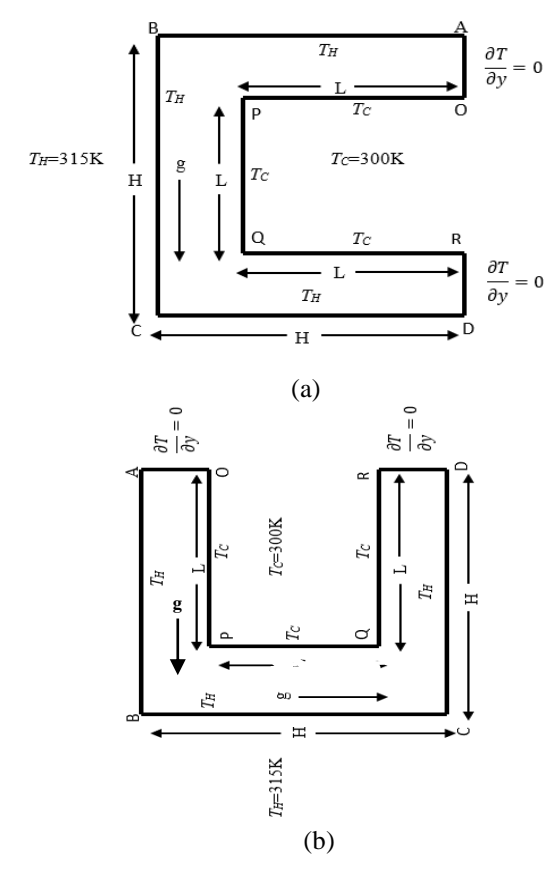


Fig. 1 Geometries of the (a) C-shaped and (b) U-shaped enclosures.

Table 1 Thermophysical properties of Air [1].

| Properties Properties | Air | | |
|-----------------------|----------|--|--|
| $C_p(j/kg k)$ | 1004.71 | | |
| $\rho(\text{kg/}m^3)$ | 1.16 | | |
| k (w/m k) | 0.0268 | | |
| $\beta(K^{-1})$ | 0.003252 | | |

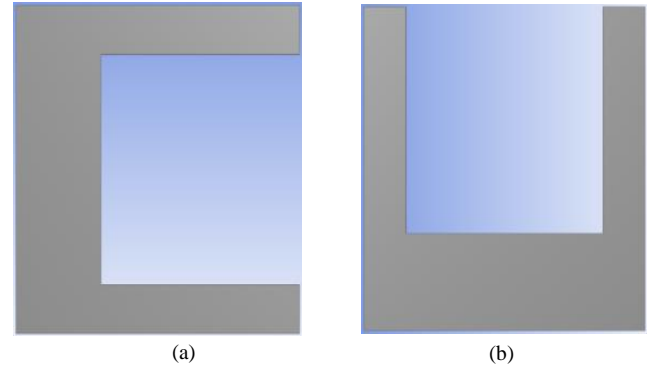


Fig. 2 Model geometry of (a) C-shape (b) U-shape enclosures.

2.2 Numerical approach and governing equations:

For the numerical approach, the dimensions of the hot walls are kept constant which is 200 mm and the dimensions of the cold and adiabatic walls were changed with

the changes of aspect ratio. A model is shown in **Fig. 2**. The aspect ratios used in this study are 0.3, 0.5, and 0.7. The Boussinesq approximation is used to make a relation between the temperature and flow field to simplify the buoyancy calculation due to the difference occurring in density in the present natural convection study.

Mesh is created using the grid size method where the element size is 0.5x0.5 mm. Thus, the enclosure contains 120000 elements after meshing shown in **Fig. 3.** The mesh independency test determines the perfect mesh size.

The solution of the natural convection flows within the U-shaped and C-shaped enclosure is governed by the following governing equations [17] and boundary conditions using the Boussinesq approximation [18].

$$\frac{\partial u}{\partial x} + \frac{\partial v}{\partial x} = 0 \tag{1}$$

$$u\frac{\partial u}{\partial x} + v\frac{\partial u}{\partial x} = \frac{1}{\rho} - \frac{\partial P}{\partial x} + (\frac{\partial^2 u}{\partial x^2} + \frac{\partial^2 u}{\partial y^2})$$
 (2)

$$u\frac{\partial v}{\partial x} + v\frac{\partial v}{\partial y} = \frac{1}{\rho}\frac{\partial P}{\partial y} + \left(\frac{\partial^2 v}{\partial x^2} + \frac{\partial^2 v}{\partial y^2}\right) + g\beta + (T$$

$$-T_0)$$
(3)

$$u\frac{\partial T}{\partial x} + v\frac{\partial T}{\partial x} = k(\frac{\partial^2 T}{\partial x^2} + \frac{\partial^2 T}{\partial x^2})$$
(4)

The finite volume approach is used to numerically solve the equations. The following boundary conditions are set for the problem:

For outer walls: u = v = 0; $T_H = 315K$ For Inner walls: u = v = 0; $T_c = 300K$ For Connecting walls: u = v = 0; $\frac{\partial T}{\partial v} = 0$

ANSYS Fluent 20.2 is used to solve this problem with converging criteria of 10^{-6} for all the governing equations with standard initialization. The process is repeated until the equations converge.

2.3 Meshing of the model and mesh Independence:

The mesh independency test for C/U-shaped enclosure is done by following the same numerical approach for aspect ratio 0.5 and various numbers of mesh/grid elements and for Rayleigh number $10^3\,.$

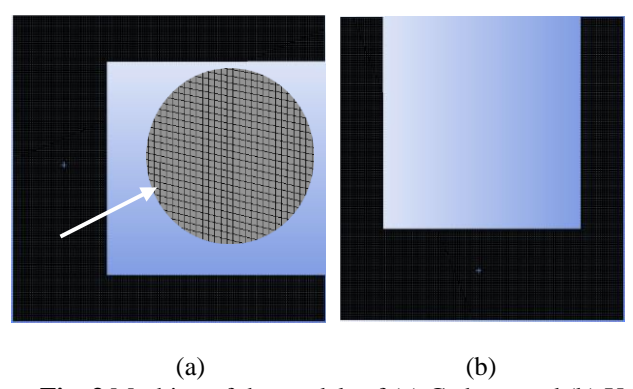


Fig. 3 Meshing of the models of (a) C-shape and (b) U-shape enclosures.

Air is filled in the enclosure for the mesh dependency test. The optimum number of mesh/grid elements is found somewhere between 50000 to 150000 which is

illustrated in **Fig. 4**. Hence, 120000 elements are chosen for this study (Element size 0.5x0.5 mm).

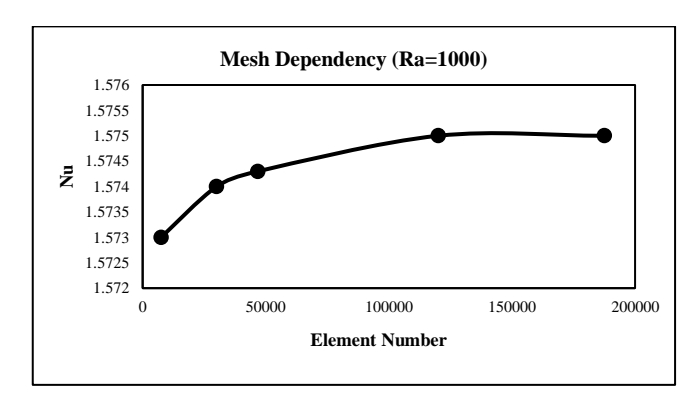


Fig. 4 Test for Mesh dependency.

2.4 Validation:

The current problem has been validated against the solutions of some works of literature shown in **Table 2**. For model validation, a square enclosure of dimension 200x200 mm is used, filled with air with a hot wall, a cold wall, and two adiabatic walls. The Nusselt number found in the literature and the present study is shown in the table for various Rayleigh numbers ranging from 10³ to 10⁶ at laminar flow regime. Since the discrepancy of the Nusselt number found in the literature and the present study tends to zero for various Rayleigh numbers, thus, it can be declared as a valid model.

Table 2 Comparison of the Nusselt number at the hot wall of the square enclosure in the current study with previous research

| Ra | Current study | Vahl Davis and Jones [19] | Khanafer et al. [20] | Billigen [21] |
|----------|---------------|---------------------------------|-------------------------|------------------|
| 10^{3} | 1.1178 | 1.118 | 1.118 | - |
| 10^{4} | 2.2468 | 2.243 | 2.245 | 2.245 |
| 10^{5} | 4.534 | 4.519 | 4.522 | 4.521 |
| 10^{6} | 8.855 | 8.799 | 8.826 | 8.800 |

3. RESULTS AND DISCUSSION:

The results presented here are for three aspect ratios of 0.3, 0.5, and 0.7, Ra ranging from 10^4 to 10^6 . The results are presented using the average Nusselt number along the hot wall, the streamline, and the temperature contour within the enclosure.

Fig. 5 illustrates temperature distribution in both C and U- shaped enclosures because of the buoyancy effects. The fluid close to the hot walls expands and density decreases. As a result, air rises near the hot walls.

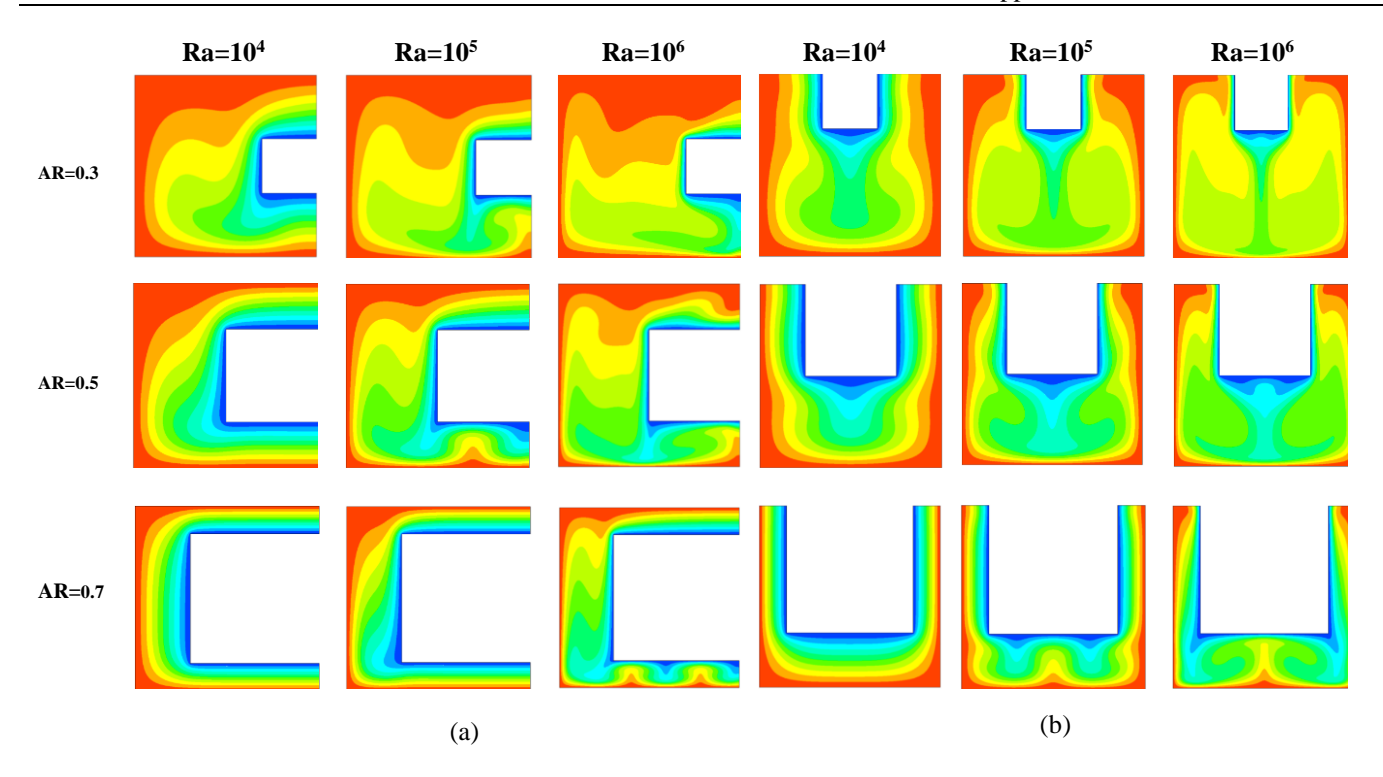


Fig. 5 Temperature Contour of (a) C-shaped and (b) U-shaped enclosure for various Ra and AR.

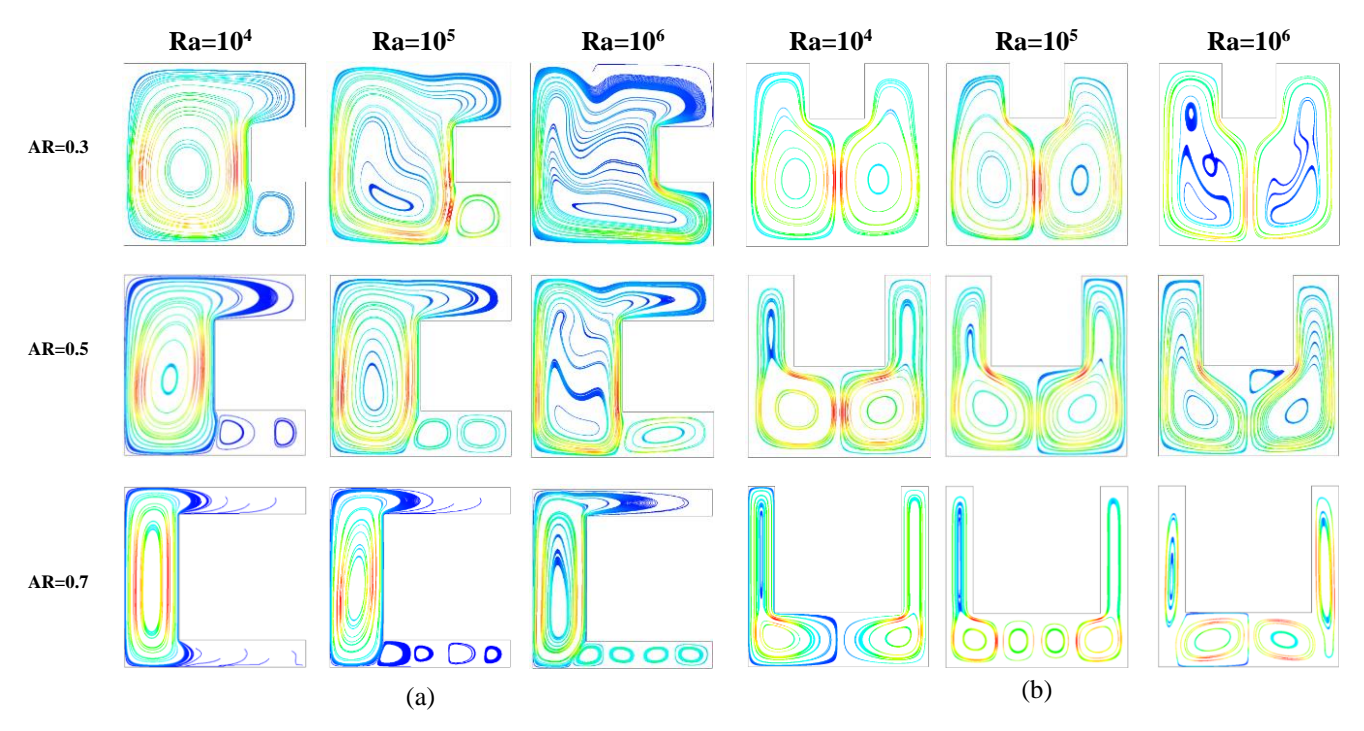


Fig. 6 Streamline of (a) C-shaped and (b) U-shaped enclosure for various Ra and AR.

Simultaneously, fluid near the cold wall moves downward because of the higher density of air compared to the hot walls. Hence, the Temperature distribution is observed. In both shapes, for any aspect ratio, an even temperature distribution is observed at lower Rayleigh numbers. The uneven temperature distribution is observed as the Rayleigh number rises, however. Owing to the cold wall's C-shaped placement, the enclosure's bottom experiences a greater region of lower temperatures, while its top experiences a

bigger higher temperature region. Lower temperature regions are observed in the center of a U-shaped enclosure due to the cold wall's placement.

Concerning any aspect ratio, temperature contour eddies in both shapes increase as the Rayleigh number rises. Both enclosures exhibit more eddies when the aspect ratio is higher.

Fig. 6 depicts the air-filled C and U-shaped enclosure's streamline for different Rayleigh numbers and aspect ratios. As the Ra gradually increases, we observe that the eddies in both the C and U shapes are more dispersed for AR=0.3. While the primary eddy forms in the center of the C-shaped enclosure, secondary eddies typically form at the bottom part of the enclosure. However, in a U-shaped enclosure, eddies usually form in the center. With increasing Rayleigh number, eddies form for AR=0.5 in a manner that is nearly identical to that of AR=0.3. But in this case, eddies seem to be more noticeable in both C and U-shaped enclosures. Here eddies form closer to the edges compared to the AR=0.3.

In the case of AR=0.7, eddy increases with the increasing Rayleigh number in both C and U-shaped enclosures. The eddies for this aspect ratio seem to be shaping better with the increasing Rayleigh number.

Fig. 7 illustrates the changes in Nusselt number with varying Rayleigh number and aspect ratio. For this particular aspect ratio, the Nusselt numbers of both shapes are nearly identical at lower Rayleigh numbers. As the Rayleigh number increases, the Nusselt number also grows. In a specific aspect ratio, the Nusselt number increases more in a U-shaped enclosure compared to a C-shaped one at higher Rayleigh numbers. For a constant Rayleigh number, the Nusselt number also increases in both shapes as the aspect ratio increases.

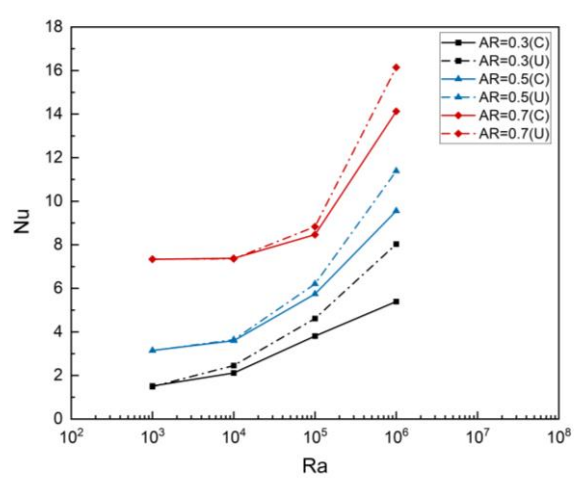


Fig. 7 The Nusselt number variation with Rayleigh number and aspect ratios for C-shaped and U-shaped enclosures.

4. CONCLUSION

This study numerically investigates the heat transfer and natural convection fluid flow in air-filled C-shaped and U-shaped enclosures, examining how the Rayleigh number, aspect ratio, and fluid properties influence flow patterns, temperature distribution, and the average Nusselt number of the heated walls. For a specific Rayleigh number, the Nusselt number increases with the aspect ratio in both enclosure shapes, with the peak Nusselt number occurring at an aspect ratio of 0.7. Additionally, higher Rayleigh numbers resulted in the formation of more eddies at a specific aspect ratio for both geometries, with the eddies exhibiting a more organized structure at elevated Rayleigh numbers. For a fixed aspect ratio, the Nusselt number rises with the Rayleigh number. However, at lower Rayleigh numbers, the heat transfer in both enclosures is

nearly identical, as indicated by similar Nusselt numbers. Interestingly, at higher Rayleigh numbers, the heat transfer in the U-shaped enclosure exceeded that of the C-shaped enclosure, as the U-shaped enclosure demonstrated a higher Nusselt number under these conditions.

References

- [1] Cengel, Y., A., Ghajar, A. J., and Kanoglu, M., "Heat and mass transfer: fundamentals and applications," 2011.
- [2] Ma, Y., Mohebbi, R., Rashidi, M. and Yang, Z., "Simulation of nanofluid natural convection in a U-shaped cavity equipped by a heating obstacle: Effect of cavity's aspect ratio," *Journal of the Taiwan Institute of Chemical Engineers*, vol. 93, pp. 263-276, 2018.
- [3] Mahmoodi, M., and Hashemi, S. M., "Numerical study of natural convection of a nanofluid in C-shaped enclosures," *International Journal of Thermal Sciences*, vol. 55, pp. 76-89, 2012.
- [4] Mohebbi, R., Izadi, M. and Chamkha, A. J., "Heat source location and natural convection in a C-shaped enclosure saturated by a nanofluid," *Physics of Fluids*, vol. 29, no. 12, 2017.
- [5] Makulati, N., Kasaeipoor, A. and Rashidi, M. "Numerical study of natural convection of a water—alumina nanofluid in inclined C-shaped enclosures under the effect of magnetic field," *Advanced Powder Technology*, vol. 27, no. 2, pp. 661-672, 2016.
- [6] Bhowmick, S., Xu, F., Molla, M. M. and Saha, S. C., "Chaotic phenomena of natural convection for water in a V-shaped enclosure," *International Journal of Thermal Sciences*, vol. 176, p. 107526, 2022.
- [7] DAVIS, G. D. V., "Laminar natural convection in an enclosed rectangular cavity," *International Journal of Heat and Mass Transfer*, vol. 11, pp. 1675-1693, 1968.
- [8] Rao, D. P. M., "A Numerical Study of Laminar Natural Convection Heat Transfer and Radiation from a Rectangular Vertical Fin Array using Quasi-3D approach," *IOSR Journal of Engineering (IOSRJEN)*, vol. 4, no. 1, 2014.
- [9] Mahmud, M. S., Rahman, M. M. and Liton, M. N. Z., "Numerical Analysis of Laminar Natural Convection Inside Enclosed Squared and Trapezoidal Cavities at Different Inclination Angles," *Journal of Engineering Advancements*, pp. 1-8, 2024.
- [10] Jassim, S. L. G., "Numerical Analysis of Laminar Natural Convection in Square Enclosure with and without Partitions and Study Effect of Partition on the Flow Pattern and Heat Transfer," *Iraqi Journal of Chemical and Petroleum Engineering*, vol. 13, no. 1, pp. 33-54, 2012.
- [11] Ghalambaz, M., Doostani, A., Izadpanahi, E. and Chamkha, A. J., "Conjugate natural convection flow of Ag–MgO/water hybrid nanofluid in a square cavity," *Journal of Thermal Analysis and Calorimetry*, vol. 139, no. 3, pp. 2321-2336, 2020.
- [12] Inam, M. I., "Direct Numerical Simulation of Laminar Natural Convection in a Square Cavity at Different Inclination Angle," *Journal of*

- Engineering Advancements, vol. 01(01), pp. 23-27, 2020.
- [13] Kent, E. F., "Numerical analysis of laminar natural convection in isosceles triangular enclosures," *Proceedings of the Institution of Mechanical Engineers, Part C: Journal of Mechanical Engineering Science*, vol. 223, no. 5, pp. 1157-1169, 2009.
- [14] Kent, E. F., "Numerical computation of laminar natural convection in triangular shaped cavities," *Adv. Appl. Mech., XIII*, vol. 128, pp. 27-38, 2020.
- [15] Chamkha, A., Ismael, M., Kasaeipoor, A., and Armaghani, T., "Entropy generation and natural convection of CuO-water nanofluid in C-shaped cavity under magnetic field," *Entropy*, vol. 18, no. 2, p. 50, 2016.
- [16] Mahmoodi, M., "Numerical simulation of free convection of a nanofluid in L-shaped cavities," *International Journal of Thermal Sciences*, vol. 50, no. 9, pp. 1731-1740, 2011.
- [17] Saleh, H., Roslan, R. and Hashim, I., "Natural convection heat transfer in a nanofluid-filled

NOMENCLATURE

- AR: Aspect ratio of the enclosure
 - T: Dimensional Temperature, K
- Ra: Rayleigh number
- K: Thermal conductivity, W/m-K
- u, v: Dimensional velocity components in x and y directions, m/s
 - H: Convective heat transfer coefficient, W/m²K
 - G: Gravitational acceleration, m/s²
- Nu: Nusselt number
- A: Thermal diffusivity, m²/s
- P: Density, kg/m³
- M: Dynamic viscosity, Pa s
- N: Kinematic viscosity, m^2/s
- B: Volumetric thermal expansion coefficient, 1/K
- H: Hot
- C: Cold

- trapezoidal enclosure," *International journal of heat and mass transfer*, vol. 54, no. 1-3, pp. 194-201, 2011.
- [18] Saha, S. C., Patterson, J. C. and Lei, C., "Natural convection in attics subject to instantaneous and ramp cooling boundary conditions," *Energy and Buildings*, vol. 42, no. 8, pp. 1192-1204, 2010.
- [19] Davis, G. de Vahl, and Jones, I., "Natural convection in a square cavity: a comparison exercise," *International Journal for numerical methods in fluids*, vol. 3, no. 3, pp. 227-248, 1983.
- [20] Khanafer, K., Vafai, K., and Lightstone, M., "Buoyancy-driven heat transfer enhancement in a two-dimensional enclosure utilizing nanofluids," *International journal of heat and mass transfer*, vol. 46, no. 19, pp. 3639-3653, 2003.
- [21] Bilgen, E., "Natural convection in cavities with a thin fin on the hot wall," *International Journal of Heat and Mass Transfer*, vol. 48, no. 17, pp. 3493-3505, 2005.